Passive Vortex Propulsion in Air: A Proof of Concept Demonstration

Nirav Surabhi
Independence High School
Ashburn, Virginia
niravsurabhi@gmail.com

Shaurya Jeevagan
Independence High School
Ashburn, Virginia
helloshaurya007@gmail.com

***Abstract*— Passive exploitation of vortex shedding has been widely studied in water, but its potential in air remains largely unexplored. This paper reports a proof-of-concept experimental demonstration showing that a rigid fin placed in the wake of a cylindrical bluff body can generate measurable forward thrust in air. A NACA 0012 fin mounted on a low-friction carriage was tested across twenty repeated trials with thrust recorded using a load cell. Results showed a mean net thrust of 3.1 N with standard deviation 0.88 N, typical peaks near 3.6 N, and root-mean-square (RMS) thrust of 2.25 N. A one-sample t-test confirmed thrust significantly greater than zero ($p < 0.001$). Nondimensional analysis yielded a thrust coefficient of 0.073 at a Reynolds number of 3.3×10^5, confirming operation in a turbulent regime. These findings provide the first evidence that passive vortex propulsion can occur in air, suggesting potential applications for energy-efficient UAVs and ground vehicle drag reduction.**

Keywords——passive propulsion, vortex-induced vibration, aerodynamic energy harvesting, bio-inspired propulsion

I. Introduction

Scientists who study hydrodynamics have performed various studies to understand how vortices that form on bodies affect objects located behind them because unstable wake patterns and oscillating flows affect both propulsion systems and energy transfer mechanisms. Nature supports different aquatic species through its environmental patterns which create opportunities for them to benefit. Fish that swim behind obstacles use periodic vortices from the obstacles to synchronize their body movements which results in lower energy consumption. This phenomenon, known as the "Kármán gait" [1], illustrates how biological systems passively harness wake energy to improve efficiency [2].

Inspired by these biological observations, numerous laboratory studies have investigated the interaction of foils or fins placed in the wakes of cylinders. These experiments have shown that downstream foils can lock into the vortex shedding frequency of the upstream bluff body, enabling them to extract momentum from the flow and, in some cases, generate net thrust [3], [4]. While these findings established a strong foundation for understanding passive propulsion, all of these demonstrations have been conducted in water, where fluid density is higher and scaling of vortex dynamics differs significantly from air.

In contrast, aerodynamic exploitation of wake energy has primarily focused on active flow-control techniques or methods to reduce drag around vehicles [5], [6], [7]. Passive thrust generation in air has received comparatively little attention, despite its potential utility. The use of passive mechanisms to capture aerodynamic wake energy would create new opportunities for UAV flight extension and micro-air vehicle endurance improvement and ground vehicle convoy fuel efficiency enhancement. The implemented strategies would achieve operational efficiency improvements while developing new bio-inspired and hybrid propulsion systems.

The authors prove through experimental data that a rigid passive fin attached to a bluff body in air air produces detectable forward motion. We describe the apparatus and experimental protocol, present results from twenty repeated trials, establish the statistical significance of the findings, and conduct nondimensional analysis in terms of thrust coefficient and Reynolds number. The research results demonstrate that passive vortex propulsion works effectively in air as well as water which confirms its potential for aerodynamic applications.

II. Experimental setup

A. Apparatus

Experiments were conducted indoors in order to minimize environmental disturbances such as wind gusts, temperature fluctuations, or uncontrolled turbulence. This is important as these factors could affect repeatability. The apparatus is shown in Fig. 1 and the fin attachment point is shown in Fig. 2. The flow was generated using a commercial handheld leaf blower. This leaf blower is rated for a nominal outlet velocity of up to 200 mph. To maximize uniformity of the blower jet and to partially condition the flow, the outlet stream was

directed through a stationary household fan. This fan acted as a coarse flow straightener. While this configuration does not produce a fully developed wind-tunnel-quality stream, it provided sufficient consistency for repeated experimental trials.

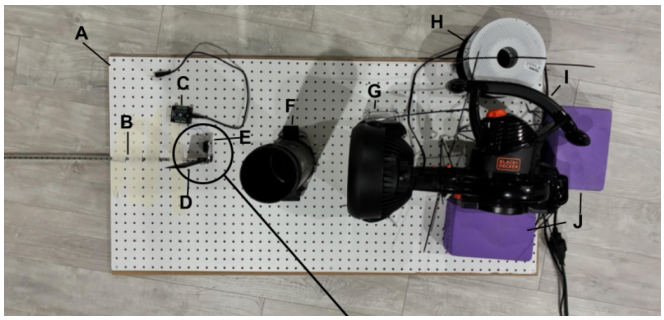

Fig. 1. Experimental apparatus. A: Pegboard level; B: MGN7 Rail; C: Load Cell Interface; D: 3D printed Fin; E: 100g Load Cell; F: Cylindrical Bluff Body; G: Circular Fan; H: Leaf-blower stand; I: Leaf-Blower; J: Foam blocks.

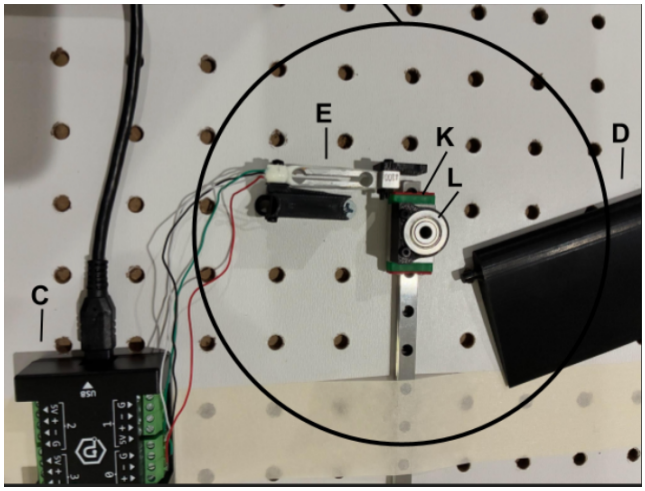

Fig. 2. Closeup of bearing and carriage with fin detached. C: Load Cell Interface; D: 3D printed Fin; E: 100g Load Cell; K: MGN7 Carriage; L: Ball bearing.

A cylindrical bluff body was mounted at the upstream end of the test section to shed a periodic Kármán vortex street. The geometry of the cylinder and its placement relative to the downstream fin were selected to promote robust vortex shedding at the Reynolds number of interest, ensuring coherent unsteady forcing on the fin.

The downstream lifting surface consisted of a rigid NACA 0012 fin with a chord length of 0.06 m, span of 0.178 m, and total planform area S = 0.0107 m². The NACA 0012 profile received selection because its symmetric design structure eliminated flow bias toward positive or negative lift during quiescent conditions which enabled thrust production through unsteady vortex interactions. The fin was mounted vertically on a low-friction rotary bearing coupled to a precision linear rail carriage (MGN7 type). The setup enabled minimal forward movement of the system while keeping unnecessary electrical resistance low so that the recorded forces mainly showed aerodynamic effects.

The carriage was positioned downstream of the load cell such that forward motion due to thrust resulted in direct contact with the sensor face, rather than being coupled through a tether. A SparkFun TAL221 bar-type load cell with a maximum rating of 100 g was used, chosen for its high sensitivity in the force range of interest (0–5 N). The carriage and fin needed to be positioned exactly 3 cm behind the load cell at the beginning of each trial to establish a fixed starting point. The controlled contact between the load cell and carriage occurred because of thrust forces which produced measurable strain that directly showed the net force. The digital acquisition system operated at 1.2 kHz to remove baseline offsets which produced thrust values that showed only dynamic aerodynamic effects without pre-loads or sensor drift.

B. Protocol

The experiments ran for 30 seconds during each trial while the blower operated continuously to maintain stable flow conditions between tests. The fin was carefully aligned in the centerline of the cylinder wake at a fixed downstream spacing, chosen to correspond with the expected formation region of a stable Kármán vortex street. The research team conducted twenty experimental trials which shared identical conditions to generate a statistically relevant data set.

To verify that the measured thrust was attributable specifically to the wake–fin interaction, two types of control tests were conducted. In the first case, the bluff body was removed and the fin alone was exposed to the blower stream.

The fin created net drag which caused the carriage to move backward by 20 cm when there was no vortex interaction. In the second case, the bluff body was present but the fin was removed; here, the carriage remained fixed at the 3 cm starting position and never contacted the load cell. These results confirmed that the positive thrust observed in the main trials required the simultaneous presence of both the bluff body and the fin.

The system added new procedures to minimize both fake vibrations and external interference. Foam damping pads were inserted at the structural mount points to suppress mechanical resonance and coupling between the blower and the linear rail assembly. The measurement system operated to detect force signals which originated from aerodynamic forces instead of structural vibrations or experimental errors.

C. Data Processing

The load cell force traces underwent baseline correction to eliminate both offset values and sensor drift effects. The researchers established active thrust windows through the identification of time periods when thrust reached more than 5% of the peak value in each trial. The statistics were obtained from areas which experienced vortex-induced forcing as the primary mechanism. The analysis included calculations of mean thrust and standard deviation and root-mean-square (RMS) thrust and peak thrust for all experimental trials. The

net propulsive effect emerged from the mean values and RMS measurements of oscillatory strength and peak values indicated the most extreme instantaneous loads.

The one-sample t-test with α = 0.05 compared each trial mean to zero to determine statistical significance. To generalize results, thrust was nondimensionalized using the thrust coefficient:

$$C_T = \frac{T}{0.5\rho U^2 S} \quad (1)$$

where T is thrust (N), ρ is air density (kg/m³), U is freestream velocity (m/s), and S is fin planform area (m²).

III. Results

A. Measured Thrust

The net thrust measurements from 20 repeated trials showed a mean value of 3.1 N while the standard deviation was 0.88 N which indicates steady operation between tests. The fin achieved its peak thrust of 3.6 N through its periodic motion which resulted in an RMS thrust of 2.25 N. The control runs produced no meaningful data because researchers confirmed that the measured forces originated from fin-wake interactions through their fin and bluff body removal tests. The results of statistical testing confirmed this finding because a one-sample t-test produced $t(19) = 15.75$ with $p < 0.001$ which proved that the mean thrust exceeded zero at a high level of statistical significance. Fig. 3 shows the mean thrust measured for each of the 20 trials, with error bars representing one standard deviation.

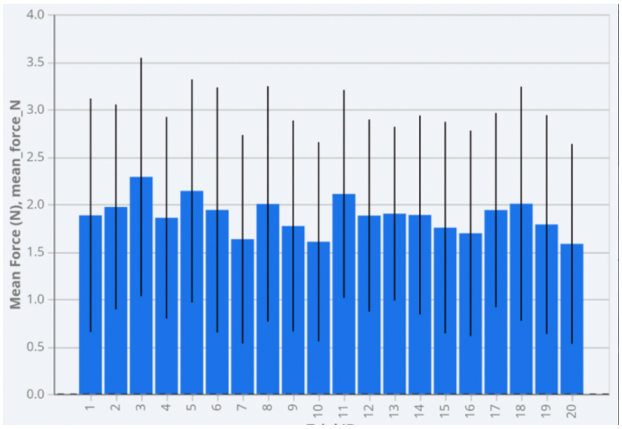

Fig. 3. Mean net thrust per trial (n=20). Dashed line indicates zero baseline.

B. Nondimensionalization

The mean thrust coefficient was calculated as $C_T = 0.073$., placing the performance in the same order of magnitude as values reported in related vortex-induced propulsion studies in water. Expressing thrust in this nondimensional form removes the dependence on the particular fin size, flow speed, or air density used in the present experiment, allowing for comparison with future studies under different conditions. In practical terms, C_T represents the fraction of the available dynamic pressure force ($0.5\rho U^2$) that is converted into useful thrust by the passive fin.

The chord-based Reynolds number was also computed as:

$$Re = \frac{\rho U c}{\mu} \quad (2)$$

where μ, the dynamic viscosity of air, is 1.81×10^{-5} Pa ·s, and c the length of the fin chord, is 0.06 m. This yielded $Re \approx 3.3\times10^5$, confirming operation within a fully turbulent aerodynamic regime. Reporting the results in terms of Reynolds number ensures that the observed behavior can be generalized beyond the present apparatus, since flows with similar Re tend to exhibit dynamically similar vortex shedding and fin response characteristics. Together, the nondimensional thrust coefficient and Reynolds number provide a framework for interpreting these findings in a broader aerodynamic context.

Representative time histories are plotted in *Fig. 4*, which overlays thrust traces from all 20 trials. Thin lines correspond to individual runs, the bold line shows the ensemble mean, and the shaded region indicates one standard deviation. The figure highlights that, despite run-to-run variation, the cycle-averaged thrust consistently remained positive.

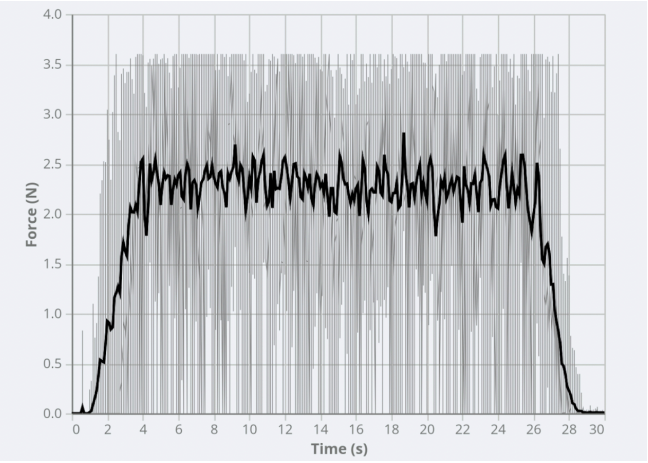

Fig. 4. Measured thrust vs. time across 20 trials. Thin lines represent individual trials. The bold line represents the mean. The shaded line shows ± 1 standard deviation.

C. Representative Time Histories

The oscillatory nature of the thrust signal is shown in more detail in *Fig. 5*, which presents a single representative trial. The trace reveals periodic peaks consistent with vortex shedding lock-in, confirming that thrust production was directly linked to unsteady wake forcing.

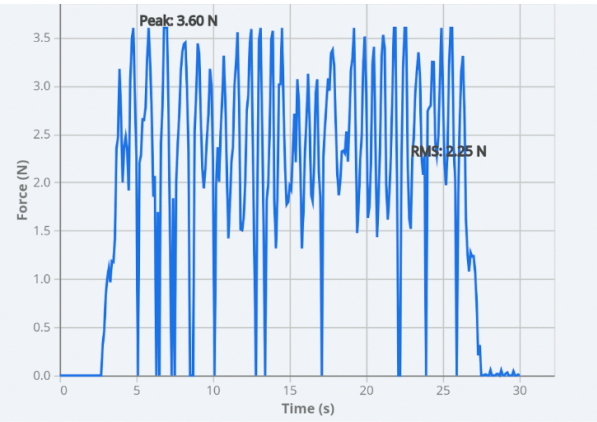

Fig. 5. Representative thrust time history for a single trial showing periodic oscillations induced by vortex shedding. Peak force is 3.60 N and RMS is 2.25 N.

IV. Discussion

The results demonstrate that passive vortex propulsion, previously reported in hydrodynamics, can also occur in aerodynamics [3], [2]. The thrust coefficient C_T of ~0.07 shows promise because the device operates with basic design yet it produces meaningful results despite being less efficient than water-based oscillating foils under perfect operating conditions [4], [10]. The research confirms that wake energy can be collected through passive air harvesting to generate forward motion according to [11] and [12].

Limitations remain. The research team chose to exclude particle image velocimetry measurements because this would have made it possible to perform Strouhal number analysis through detailed flow characterization. Such analysis would be valuable because the timing of vortex shedding relative to the fin's motion is known to critically affect propulsive performance [13]. The proof-of-concept implemented consumer-grade instruments which produced measurement uncertainties, but future research needs to employ research-grade force balances for improved results. The fin geometry was not varied, so generalization to different stiffnesses, spans, and gap ratios is untested. Research conducted earlier shows that flexible foils help generate better thrust output [14] and scientists found the best distance between cylinders and foils for maximum thrust generation [15]. Nonetheless, the statistical strength of the results ($p < 0.001$) confirms the phenomenon.

The technology has potential uses for truck and UAV trailing appendages which help reduce wake losses according to [8] and [9]. The system-level advantages need assessment of drag increase effects together with structural limitations which impact the system. Research should focus on understanding how fin stiffness and geometry affect experimental outcomes [14] [16] and PIV should be used to analyze vortex–fin interactions in depth [17]. The design of efficient aerodynamic systems that harness passive wake energy should draw inspiration from flapping foils [18], [19] and hybrid vortex-control strategies [10].

V. Conclusion

This study provides the first aerodynamic demonstration of passive vortex propulsion. The rigid fin which entered the bluff-body wake produced a mean thrust force of 3.1 N ($C \approx 0.073$) at $\mathrm{Re} \approx 3.3\times10^5$ during twenty consecutive trials. The research expands passive wake-energy harvesting from water-based systems to air-based systems while creating opportunities to study this technology with enhanced measurement tools and visual analysis and different geometric configurations.

Acknowledgment

The authors declare that this research received no external funding.

References

[1] J. C. Liao, "A review of fish swimming mechanics and behaviour in altered flows," *Philosophical Transactions of the Royal Society B*, vol. 362, no. 1487, pp. 1973–1993, 2007.

[2] J. C. Liao, D. N. Beal, G. V. Lauder, and M. S. Triantafyllou, "Fish exploiting vortices decrease muscle activity," *Science*, vol. 302, pp. 1566–1569, 2003.

[3] D. N. Beal, F. S. Hover, M. S. Triantafyllou, J. C. Liao, and G. V. Lauder, "Passive propulsion in vortex wakes," *Journal of Fluid Mechanics*, vol. 549, pp. 385–402, Feb. 2006.

[4] J. M. Anderson, K. Streitlien, D. S. Barrett, and M. S. Triantafyllou, "Oscillating foils of high propulsive efficiency," *Journal of Fluid Mechanics*, vol. 360, pp. 41–72, 1998.

[5] F. E. Fish and G. V. Lauder, "Passive and active flow control by swimming fishes and mammals," *Annual Review of Fluid Mechanics*, vol. 38, pp. 193–224, Jan. 2006.

[6] M. G. Connolly, A. Ivankovic, and M. J. O'Rourke, "Drag reduction technology and devices for road vehicles – a comprehensive review," *Heliyon*, vol. 10, no. 13, e33757, 2024.

[7] H. Weimerskirch, J. Martin, Y. Clerquin, P. Alexandre, and S. Jiraskova, "Energy saving in flight formation," *Nature*, vol. 413, pp. 697–698, 2001.

[8] C. Bonnet and H. Fritz, "Fuel consumption reduction in a platoon: Experimental results with two electronically coupled trucks at close spacing," SAE Tech. Paper 2000-01-3056, 2000.

[9] H. Choi, W.-P. Jeon, and J. Kim, "Control of flow over bluff bodies," *Annual Review of Fluid Mechanics*, vol. 40, pp. 113–139, 2008.

[10] X. Shao, D. Pan, J. Deng, and Z. Yu, "Hydrodynamic performance of a fishlike undulating foil in the wake of a cylinder," *Physics of Fluids*, vol. 22, no. 11, 111903, 2010.

[11] K. Shoele and Q. Zhu, "Fluid–structure interaction simulation on energy harvesting from a vibrating cylinder using a fully passive flapping foil," *Journal of Fluids Engineering*, vol. 140, no. 1, p. 011105, 2018.

[12] D. Iverson, M. Rahimpour, W. Lee, T. Kiwata, and P. Oshkai, "Effect of chordwise flexibility on propulsive performance of high-inertia oscillating foils," *Journal of Fluids and Structures*, vol. 91, p. 102750, 2019

[13] C. H. K. Williamson and R. Govardhan, "Vortex-induced vibrations," *Annual Review of Fluid Mechanics*, vol. 36, pp. 413–455, 2004.

[14] J. N. Lefebvre and A. R. Jones, "Experimental investigation of airfoil performance in the wake of a circular cylinder," *AIAA Journal*, vol. 57, no. 7, pp. 2808–2818, 2019.

[15] J. Li, P. Wang, X. An, D. Lyu, R. He, and B. Zhang, “Investigation on hydrodynamic performance of flapping foil interacting with oncoming von Kármán wake of a D-section cylinder,” *Journal of Marine Science and Engineering*, vol. 9, no. 6, p. 658, 2021.

[16] Y. Bao and J. Tao, “Dynamic reactions of a free-pitching foil to the reverse Kármán vortices,” *Physics of Fluids*, vol. 26, no. 3, 031704, 2014.

[17] K. Streitlien, G. S. Triantafyllou, and M. S. Triantafyllou, “Efficient foil propulsion through vortex control,” *AIAA Journal*, vol. 34, no. 11, pp. 2315–2319, 1996.

[18] E. G. Drucker and G. V. Lauder, “Locomotor forces on a swimming fish: Three-dimensional vortex wake dynamics quantified using digital particle image velocimetry,” *Journal of Experimental Biology*, vol. 202, no. 18, pp. 2393–2412, 1999.

[19] J. J. Allen and A. J. Smits, “Energy harvesting eel,” *Journal of Fluids and Structures*, vol. 15, no. 3–4, pp. 629–640, 2001.